Dyes and Pigments 95 (2012) 260–267

Contents lists available at SciVerse ScienceDirect

Dyes and Pigments

journal homepage: www.elsevier.com/locate/dyepig

The synthesis, morphology and liquid-crystalline property of polysiloxane-modified perylene derivative

Yan Liang, Hua Wang, Dengxu Wang, Hailong Liu, Shengyu Feng*

Key Laboratory of Special Functional Aggregated Materials, Ministry of Education, School of Chemistry and Chemical Engineering, Shandong University, Jinan 250100, People's Republic of China

ARTICLE INFO

Article history:
Received 15 February 2012
Received in revised form
27 April 2012
Accepted 30 April 2012
Available online 9 May 2012

Keywords:
$\pi-\pi^*$ stacking
Liquid-crystalline
Morphology
Perylene derivative
Polysiloxane
Synthesis

ABSTRACT

A novel polysiloxane-modified perylene derivative was designed and synthesized through the amidation reaction between aminopropyl-terminal polysiloxane and perylene tetracarboxylic diester monoimides with *n*-dodecyl as the alkyl chain connected to the perylene core. The synthesized compound was subjected to IR and ^{1}H NMR. The liquid-crystalline property of the modified perylene derivative at room temperature (ranged from 27.1 °C to 61.3 °C) was characterized via differential scanning calorimetry, polarization optical microscope, X-ray powder diffraction, and small-angle X-ray scattering. The morphology of the compound was evaluated via scanning electron microscopy and atomic force microscopy in tapping mode. The static contact angle of the perylene derivative with distilled water as the test liquid was improved after modification by polysiloxane. All the measurements revealed that the polysiloxane-modified perylene derivative exhibited good thermal stability, excellent optical property, good hydrophobic property, and low temperature liquid-crystalline property. These properties may be attributed to the presence of flexible Si–O–Si chain and ordered $\pi-\pi^*$ stacking between adjacent perylene cores.

1. Introduction

Based on their large π-conjugated system, perylene derivatives possess excellent chemical, thermal, and optical stabilities, as well as broad spectrum absorption and photoconductive properties. Furthermore, perylene derivatives can be self-assembled to form a liquid-crystalline phase [1]. Therefore, they are widely used as organic light emitting diodes, fluorescent chemosensors, liquid crystal displays, organic solar cells, and organic field-effect transistors [2–6].

The liquid-crystallized property of perylene and its derivatives is induced by the parallel $\pi-\pi^*$ stacking between neighboring perylene cores [7]. Previous studies have reported that liquid-crystalline perylene derivatives are centered on perylene bisimides (PBI) and perylene tetra-(alkoxycarbonyl) (PTAC) [8,9]. PBI is widely used as a liquid-crystalline material, an *n*-type semiconductor for the strong $\pi-\pi^*$ stacking of perylene cores, and a good electron acceptor for its high electron affinity [10,11]. However, PBI materials exhibit poor processability, which is considered a disadvantage and thereby limits their application [12]. Moreover, materials containing PTAC with an alkyl substituent connected to the perylene core show good processability, excellent fluorescence and exhibit liquid-crystalline property [13]. The alkyl chain connected to the perylene core enhances the solubility of perylene derivatives, particularly in solution [14]. This enhancing effect can be attributed to the presence of a long chain with decreased charge intensity in PTAC. However, increasing the chain length of the substituent prevents $\pi-\pi^*$ stacking, thereby affecting the liquid-crystalline property [8]. A novel polymer-modified perylene derivative synthesized using polyethylenimines (PEIs; with an imide and two ester groups connected to the same perylene cores) and polymers was developed to overcome the disadvantages posed by PBI and PTAC [15,16]. The modified perylene derivative with a large substituent demonstrated good processability and exhibited liquid-crystalline and semi-conducting properties, which can be used in broader applications in the future [17]. Current reports on polymer-modified perylene have focused on carbon-chain compounds. However, polysiloxane used in the reaction with PEIs has not yet been studied. It is well known that polysiloxane possesses many specific properties, including good hydrophobic property, high flexibility of the main chains, low glass transition temperature, good processability, and excellent thermal stability [18]. Thus, a polysiloxane-modified perylene derivative likely exhibits new properties.

* Corresponding author. Tel.: +86 531 88364866; fax: +86 531 88564464.
E-mail address: fsy@sdu.edu.cn (S. Feng).

0143-7208/$ – see front matter © 2012 Elsevier Ltd. All rights reserved.
doi:10.1016/j.dyepig.2012.04.015

In the current study, we synthesized a novel polysiloxane-modified perylene derivative with good fluorescence property, excellent hydrophobic performance, and good liquid-crystalline property. An acid-catalyzed route with high productivity was used to transfer PTAC to PEIs [17]. The aminopropyl-terminal polysiloxane was used to react with PEIs and obtain the modified perylene derivative. The *n*-dodecyl group in PEIs was used to connect to the perylene core to achieve good solubility. Additionally, differential scanning calorimetry (DSC), polarization optical microscope (POM), contact angle analyzer, X-ray powder diffraction (XRD), and small-angle X-ray scattering (SAXS) were used to measured the hydrophobic liquid-crystalline properties. The film morphology by scanning electron microscope (SEM) and atomic force microscope (AFM) in tapping mode was also described.

2. Experiments

2.1. Materials

The starting materials, 3,4,9,10-perylene tetracarboxylic dianhydride, 1-bromododecane, *n*-dodecane, potassium hydroxide and solvents were purchased from China National Medicines Group. Solvents were distilled before used. Aliquant 336 was obtained from Aldrich and used without further purification. Aminopropyl-terminal polysiloxane was purchased from Fangzhou chemical material company and used without further purification.

2.2. Measurements

^{1}H NMR was recorded on a Bruker-AVANCE 400 NMR Spectrometer with $CDCl_3$ as the solvent without tetramethylsilane (TMS) as an internal reference. Infrared measurements with the KBr pellet technique were performed within the 4000–400 cm^{-1} region on a Bruker TENSOR-27 FTIR spectrometer. The fluorescence spectrum (excitation and emission) data were measured by HITACHI F-4500 spectrophotometer. Ultraviolet absorption (UV) spectra of these samples (in $CHCl_3$ solution) were recorded using a Hitachi U-4100 spectrometer. TGA was obtained by STA 449 F3 (NETZSCH) with heating rate of 10 °C/min under N_2 condition from room temperature to 600 °C at ambient pressure. DSC (α-Al_2O_3 as reference material) was measured by Mettler Toledo DSC822 series with a heating rate of 10 °C/min under nitrogen flow of 30 mL/min from −30 to 200 °C. POM was performed on a BX-51 polarization optical microscope (Olympus, Japan) with a heating rate of 1 °C/min. Static contact angles were measured with the sessile drop method by a Dataphysics OCA-20 contact angle analyzer with distilled water as the test liquid. The X-ray powder diffraction data was carried out on powered samples via BRUKER D8 diffraction (40 mA, 40 kv) using monochromator Cu Kα radiation ($\lambda = 1.54$ Å) over the 2θ range of 1° to 50°. Small-angle X-ray scattering data were characterized by an HMBG-SAX X-ray small-angle scattering system (Austria) with a Ni-filtered Cu Kα radiation (0.154 nm) operating at 25 kV and 20 mA. The distance between the detector and the sample was 27.8 cm. The AFM was measured by using a NanoScoPe IIIA multimode atomic force microscope under ambient condition in tapping mode. The morphology was measured by Zeiss Supra 55 Scanning Electron Microscope.

2.3. Synthesis

2.3.1. 3,4,9,10-Tetra(dodecyloxycarbonyl) perylene (PTDC)

3,4,9,10-Perylene tetracarboxyl dianhydride (1.96 g, 5 mmol) was dissolved in 100 mL KOH (0.1 mol/L) solution and stirred at 70 °C for 0.5 h. The solution was filtrated, and the pH value of the filtrate was adjusted to 8–9 using 1 M HCl. 1-Bromododecane (9.97 g, 40 mmol) was added into the solution after Aliquat 336 (2 g) and KI (0.125 g, 1 mmol) were charged into the solution and stirred vigorously for 10 min. The mixture was refluxed for 10 h until red oil floated on the top and the bottom layer of the solution became clear. Subsequently, chloroform was poured into the mixture, and the chloroform phase layer was washed thrice with 15% aqueous sodium chloride solution. A yellow solid was obtained by adding ethanol into the concentrated chloroform solution and dried under vacuum condition at 80 °C [19]. IR (KBr pellet, cm^{-1}): $\nu = 2924$ (antisymmetric CH_2), 2845 (symmetric CH_2), 1725 (anhydride C=O), 1606 (aromatic ring stretch). ^{1}H NMR (400 MHz $CDCl_3$, ppm): δ 8.3 (4H, Ar–**H**), 8.0 (4H, Ar–**H**), 4.3 (8H, (COO)C**H**$_2$), 1.8 (8H, (COO)CH_2C**H**$_2$), 1.4 (8H, (COO)CH_2CH_2C**H**$_2$), 1.2 (64H, (COO)$CH_2CH_2CH_2$(C**H**$_2$)$_8$), 0.8 (12H, CH_2C**H**$_3$) (Scheme 1).

2.3.2. Perylene-3,4-anhydride-9,10-di-(dodecyloxycarbonyl) (PADC)

PTDC (0.88 g, 0.8 mmol) was charged into a 25 mL round-bottom flask with 2.5 mL *n*-dodecane and 0.5 mL toluene before

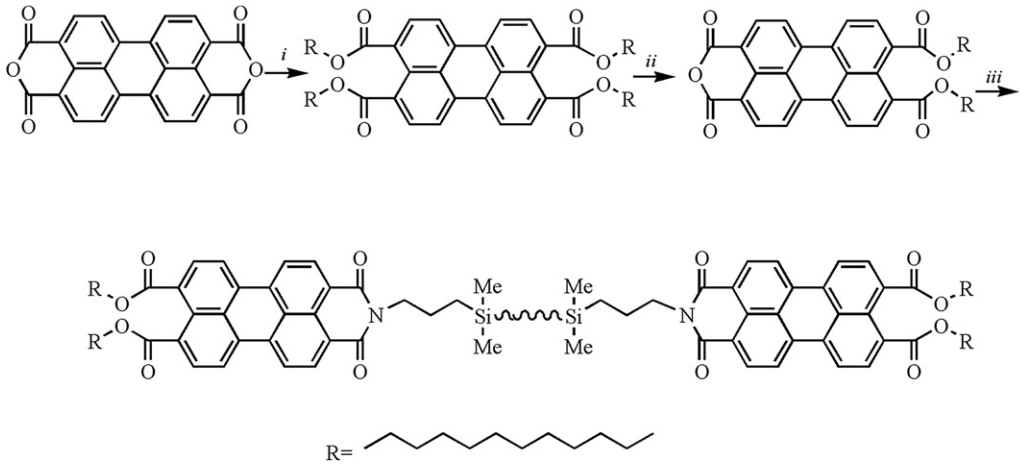

Scheme 1. Synthesis of perylene-9,10-di-(dodecyloxycarbonyl) terminal polysiloxane (PCTP).

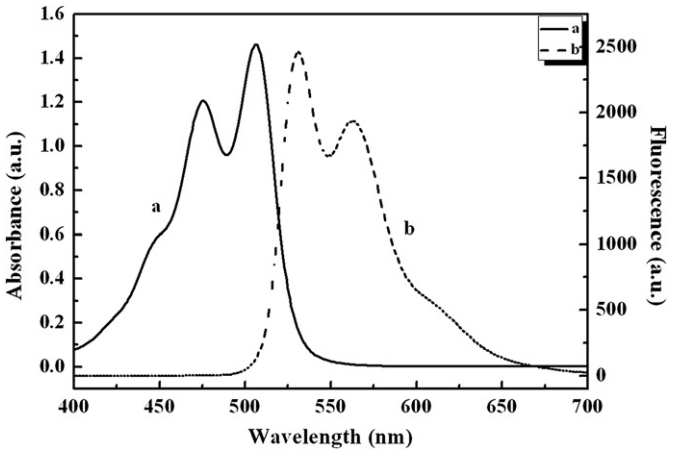

Fig. 1. (a) UV–vis spectra and (b) fluorescence spectra of PCTP measured in $CHCl_3$ at 10^{-6} M (excitation wavelength was 505 nm).

heating to 95 °C. After the yellow product was completely dissolved, *p*-toluenesulfonic acid monohydrate (0.13 g, 0.8 mmol) was added to the solution and maintained at 95 °C for 5 h. The mixture was dissolved in chloroform and added with 300 mL methanol to allow the red deposition to precipitate. The deposition was washed repeatedly with ethanol until the filtrate became colorless and then purified via column chromatography, with $CHCl_3$/acetone (v/v: 20/1) as the eluent [9]. Yield: 70% as a red solid (Mp >268.5 °C). IR (KBr pellet, cm^{-1}): $\nu = 2925$ (antisymmetric CH_2), 2853 (symmetric CH_2), 1769 (anhydride C=O), 1722 (ester C=O), 1589 (aromatic ring stretch). ^1H NMR (400 MHz $CDCl_3$, ppm): δ 8.68 (2H, Ar–**H**), 8.56 (4H, Ar–**H**), 8.15 (2H, Ar–**H**) 4.36 (4H, (COO)C**H**$_2$), 1.82 (4H, (COO)CH_2C**H**$_2$), 1.44 (4H, (COO)CH_2CH_2C**H**$_2$), 1.25 (32H, (COO)$CH_2CH_2CH_2$(C**H**$_2$)$_8$), 0.87 (6H, CH_2C**H**$_3$) (Scheme 1).

2.3.3. Perylene-9,10-di-(dodecyloxycarbonyl) terminal polysiloxane (PCTP)

Molten imidazole is an excellent solvent for the imidization reaction of perylene anhydrides. Hence, PADC and imidazole were charged into a three-necked flask with a reflux condenser, a constant pressure dropping funnel, and a nitrogen inlet, and then heated to 120 °C [17]. Consequently, aminopropyl-terminal polysiloxane with a molecular weight of 2000 g/mol was added into the mixture. The temperature of the mixture was maintained at 120 °C for 5 h. Subsequently, the reaction mixture was cooled to 90 °C and poured into 30 mL of water. All the processes were carried out under argon atmosphere, and the crude product was collected via centrifugation. The crude product was purified using 5 mL ether [85% yield as a red solid (Mp: 60.4 °C)]. IR (KBr pellet, cm^{-1}): $\nu = 2921$ (antisymmetric CH_2), 2851 (symmetric CH_2), 1772 (imide C=O), 1712 (ester C=O), 1593 (aromatic ring stretch).^1H NMR (400 MHz $CDCl_3$, ppm): δ 8.60 (4H, Ar–**H**), 8.42 (8H, Ar–**H**), 8.10 (4H, Ar–**H**) 4.37 (8H, (COO)C**H**$_2$), 4.22 (4H, Si–C**H**$_2CH_2CH_2$), 1.84 (8H, (COO)CH_2C**H**$_2$), 1.48 (8H, (COO)CH_2CH_2C**H**$_2$), 1.28 (64H, (COO)$CH_2CH_2CH_2$(C**H**$_2$)$_8$), 1.17 (4H, $SiCH_2$–C**H**$_2$), 0.88 (12H, CH_2C**H**$_3$), 0.74 (4H, $SiCH_2CH_2$-C**H**$_2$), 0.09 (180H, Si–C**H**$_3$) (Scheme 1).

3. Results and discussion

3.1. Optical properties

The chloroform solution containing PCTP exhibited a bright golden-yellow fluorescence even under daylight condition. The absorption and fluorescence spectra of PCTP at a low concentration in chloroform are shown in Fig. 1. The absorption revealed two absorbance peaks at 475 and 506 nm, indicating a weak shoulder similar to π–π^* transitions that correspond to $S_1 \rightarrow S_2$, $S_0 \rightarrow S_1$, and $S_0 \rightarrow S_2$ transitions [19,20]. Fig. 1 also shows that the fluorescence spectrum exhibited a mirror image corresponding to the UV–Vis spectrum. The spectrum revealed two pronounced peaks centered at 530 and 561 nm, and one weak shoulder centered at 611 nm. Compared with the absorption and fluorescence of aminopropyl-terminal polysiloxane (ATP) in our previous report, PCTP showed an excellent fluorescence property that could be applied in the optoelectronic field [21].

Studies have reported that the liquid-crystalline property caused by the parallel π–π^* stacking between neighboring perylene cores can lead to a new absorption peak at 570 nm. However, the absorption spectrum of PCTP showed no absorption peak at approximately 570 nm because of the existence of a large substituent [7]. Müllen and Schferäfer explained the phenomenon of PTAC with a large substituent attached at the bay region [22,23]. They believe that the large substituent is perpendicular to the flat perylene core and decreases the chance of π–π^* stacking between neighboring perylene cores. Our results suggest that the small probability of π–π^* stacking may be attributed to the steric hindrance in the large substituent or the low concentration, which agrees with the previous study [24].

3.2. Thermotropic properties

The thermal stability of PADC, PCTP, and ATP was investigated using thermogravimetric analysis at a heating rate of 10 °C/min from room temperature to 600 °C under N_2 and air (100 mL/min),

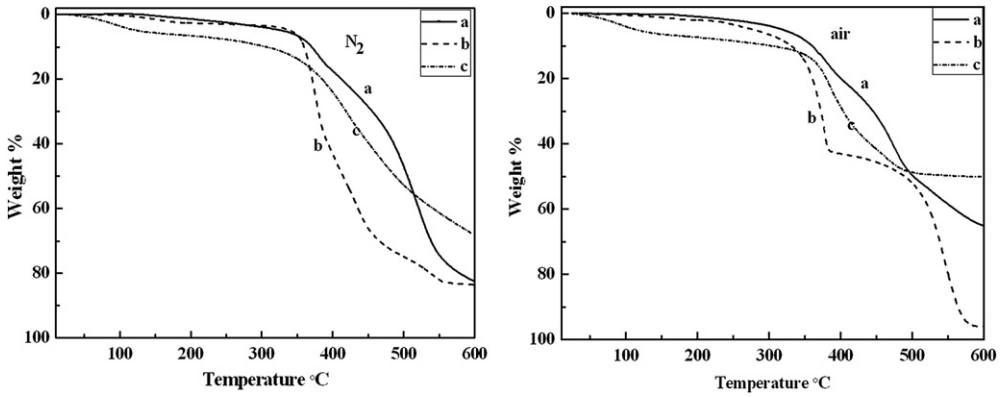

Fig. 2. Thermal degradation of (a) PCTP, (b) PADC and (c) ATP from room temperature to 600 °C with heating rate of 10 °C/min under N_2 and air, respectively.

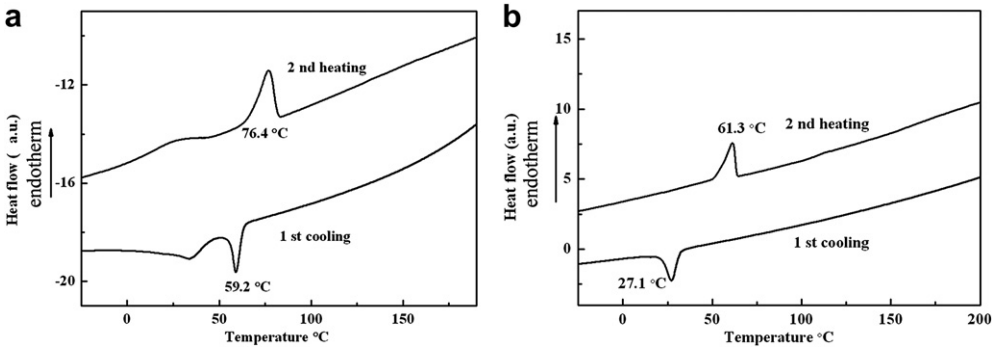

Fig. 3. DSC thermograms of (a) PADC and (b) PCTP with heating rate of 10 °C/min under N_2 condition.

Table 1
Phase behavior of PADC and PCTP obtained from DSC.

Phase transitions and corresponding enthalpies ΔH		
	Second heating cycle (T/°C; ΔH/J g^{-1})	First cooling cycle (T/°C; ΔH/J g^{-1}))
PADC	Phase transition of alky chain (75.4 °C; 2.39)	Phase transition of alky chain (59.2 °C; 1.18)
PCTP	LC (61.3 °C; 1.91) → I	I (27.1 °C; 1.94) → LC

LC, liquid-crystalline; and I, isotropic.

respectively. As shown in Fig. 2, the thermal stability of PADC showed a resemblance with PCTP before the sharp decline appeared at 349 °C. However, PCTP exhibited a good thermal stability from the beginning to the end of the reaction under N_2 condition. This result can be attributed to the presence of Si—O—Si, which greatly improved the thermal stability of the perylene derivative. Furthermore, PCTP showed the best thermal stability under ambient air. A platform was developed for the compound PADC under ambient air because the alkyl chain was lost at approximately 400 °C [16,25]. Compared with PADC and PCTP, ATP exhibited the worst thermal stability at a temperature lower than 400 °C. The results indicated that utilizing polysiloxane to modify perylene derivatives can significantly improve the thermal stability of the raw material. Therefore, the modified perylene derivative can be used as a high-temperature material.

DSC thermograms were measured at a heating rate of 10 °C/min under N_2 condition, and the results are shown in Fig. 3. Phase transition temperature and the corresponding enthalpies are summarized in Table 1. The first heating cycles were not considered because of the effect of initial thermal condition. Fig. 3(a) shows a phase transitions at 76.4 °C for PADC, respectively. The melting point of PADC was above 268 °C. Hence, the phase transition at 76.4 °C should be attributed to the amorphous carbon chain. The corresponding peak was discovered at 59.2 °C after cooling. Only one reversible phase transition (61.3 °C) was observed in PCTP using DSC, and the crystallization temperature was found at 27.1 °C [12]. According to DSC data, imperfections fan-shaped textures of PTCP can be obtained using POM [Fig. 4(b)] at 60 °C. The POM image of PADC at the same temperature is shown in Fig. 4(a). Based on the observation, PTCP exhibited liquid-crystalline property at the same temperature.

3.3. Contact angle analysis

Static contact angle analysis was performed to study the effect of polysiloxane on hydrophobic performance. PADC and PCTP were initially dissolved in chloroform and then deposited on glasses using a whirler. The image of the drop was calculated from the shape of the drop (both left and right contact angles) with an accuracy of ±0.1° using an image analysis system. Distilled water was used as the test liquid. All measurements were conducted at 25 °C. Polysiloxane is usually applied as a hydrophobic material because it exhibits a water contract angle of approximately 109° ± 0.1° [26]. Fig. 5(a) shows that PADC exhibited a water contract angle of approximately 100° ± 0.1°. Compared with PDMS and PADC, the contact angle of PCTP [Fig. 5(b)] was 112° ± 0.1°. This result indicates that the excellent hydrophobic property of the

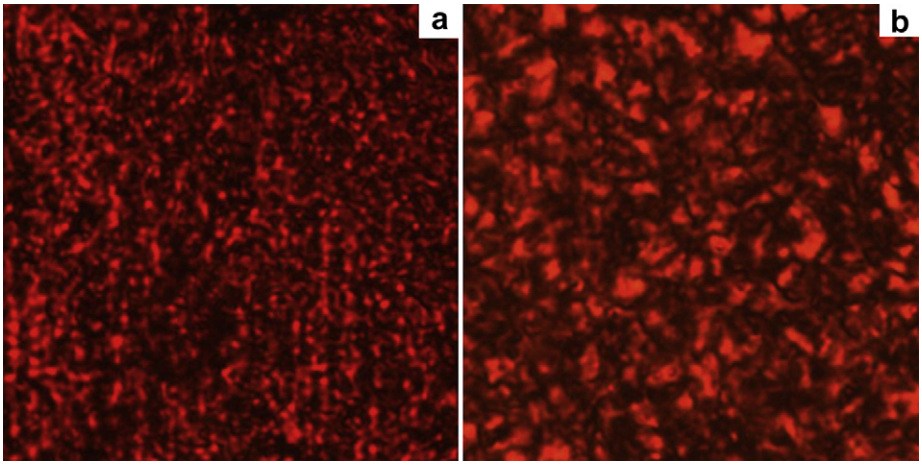

Fig. 4. Polarization optical microscope images of (a) PADC and (b) PCTP at 60 °C.

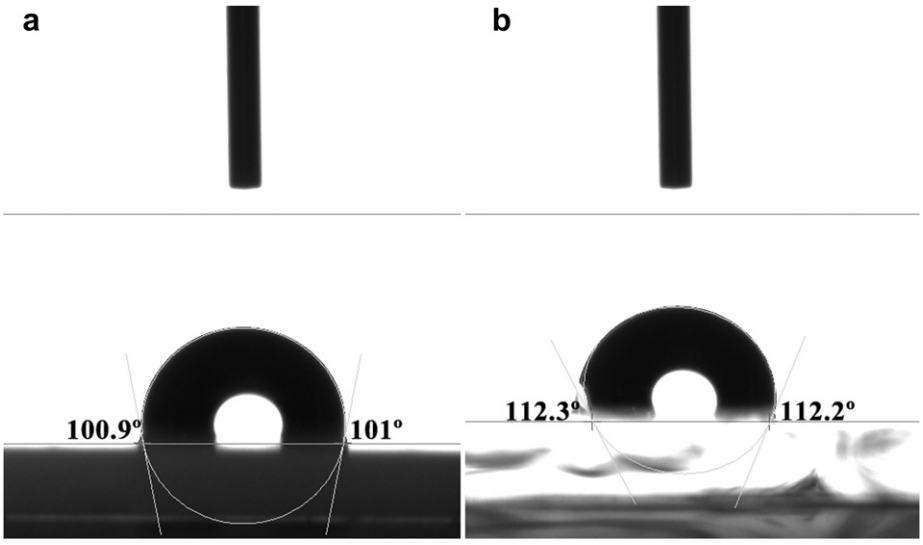

Fig. 5. Contact angle images of (a) PADC and (b) PCTP.

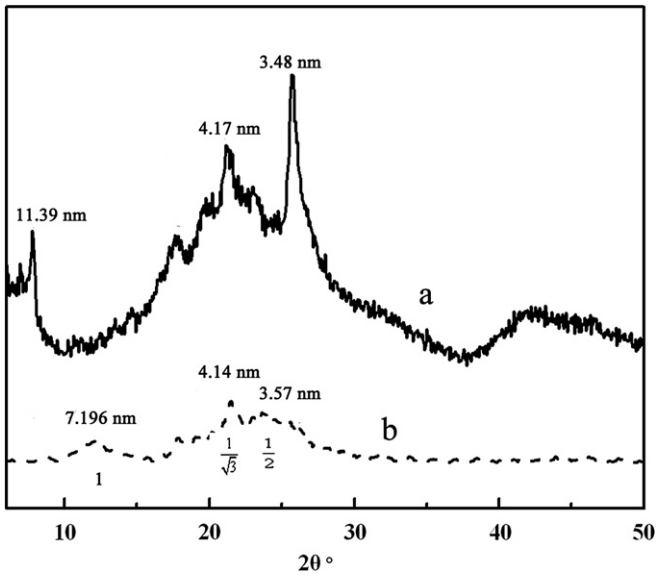

Fig. 6. X-ray powder diffraction of (a) PADC and (b) PCTP at room temperature (29 °C).

compound can be attributed to the integration of perylene and Si–O–Si bonds.

3.4. X-ray powder diffraction (XRD) and small-angle X-ray scattering (SAXS)

The liquid-crystalline characters of the powder samples were collected using both X-ray powder diffraction measurement and SAXS geometries to verify the crystalline behavior of PADC and PCTP. The data from XRD were measured with a 2θ range of 1° to 50° at room temperature (29 °C). The XRD data of PADC [Fig. 6(a)] revealed three sharp reflection peaks. The peak at 25.6° corresponding to a *d* space of 3.48 Å can be attributed to the $\pi-\pi^*$ stacking of the adjacent perylene because the distances of $\pi-\pi^*$ stacking between the perylene cores were approximately 3.5 Å [27,28]. The sharp peak at approximately 21.24° corresponding to a *d* space of 4.17 Å can be ascribed to the dislocation of $\pi-\pi^*$ stacking of perylene. Perylene derivatives are well known to exhibit a typical sharp diffraction peak at approximately 8–9°, which is centered at a peak of 7.17° in curve a [29]. Compared with PADC, the peak at 7.17° shifted to 7.75° with *d* space of 7.196 Å after the perylene derivative modified by polysiloxane (curve b). The corresponding *d* spaces changed to 4.14 and 3.57 Å as the peaks shifted to 21.56° and 25.12° for PCTP, respectively. Although the

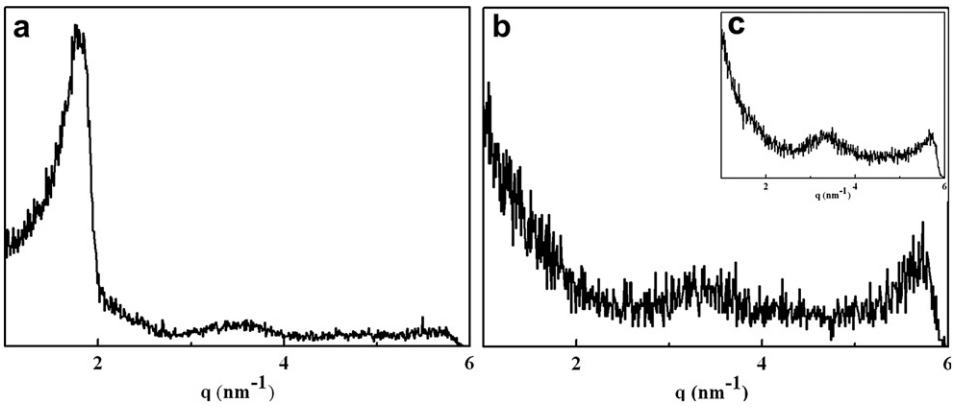

Fig. 7. Small-angle X-ray scattering at room temperature (25 °C) of (a) PADC and (b) PCTP; (c) small-angle X-ray scattering of PCTP at 55 °C.

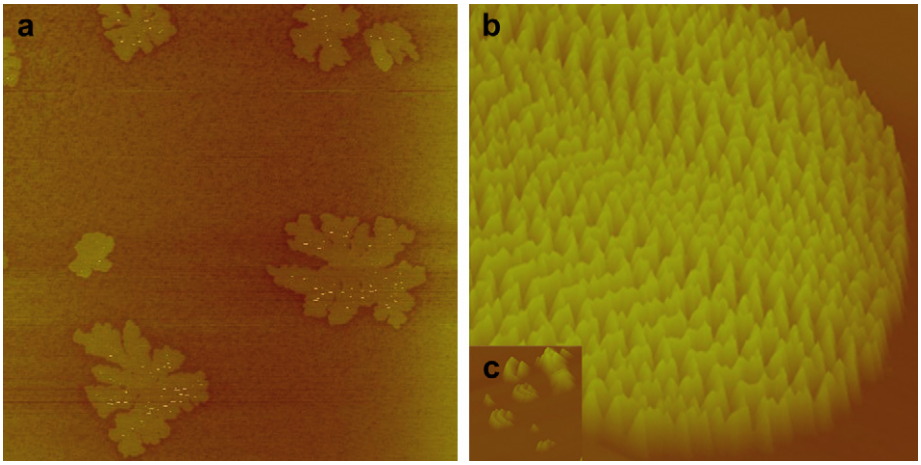

Fig. 8. AFM images of PADC (a), PCTP (b) and the partial enlarged drawing of PCTP (c).

perylene content in PCTP decreased, it still exhibited $\pi-\pi^*$ stacking at room temperature. Additionally, the typical rations of $1 : 1/\sqrt{3} : 1/2$ for the d spacing estimated from Bragg reflection were in accordance with a hexagonal lattice [30]. The SAXS result of PADC revealed a sharp peak at $q = 1.7955\ \mathrm{nm}^{-1}$, which corresponds to perylene [Fig. 7(a)]. The content of perylene decreased after modification by polysiloxane, which also agrees with the SAXS data of PTCP [Fig. 7(b)], wherein the sharp peak disappeared and two broad peaks appeared. The broad peaks distinctly appeared when the sample was heated to 55 °C [Fig. 7(C)]. In addition, the peak position ratio was $1 : \sqrt{3}$, which corresponds to a hexagonal lattice [31,32].

3.5. Film morphology

The morphology of the compounds was further characterized using the tapping mode of atomic force microscopy (AFM) and scanning electron microscopy (SEM). The AFM images of PADC and PCTP are shown in Fig. 8. The crystal phase of PADC with a concentration of 10^{-6} mol/L in chloroform solvent [Fig. 8(a)] was observed after drop casting on the mica substrate. A single-layer was formed at this concentration, with a layer thickness of approximately 0.733 nm to 0.773 nm, which is approximately close to the molecular layer distance of crystalline perylene (1.01 nm) with a standard error value of ±0.2 nm for the AFM scans [33].

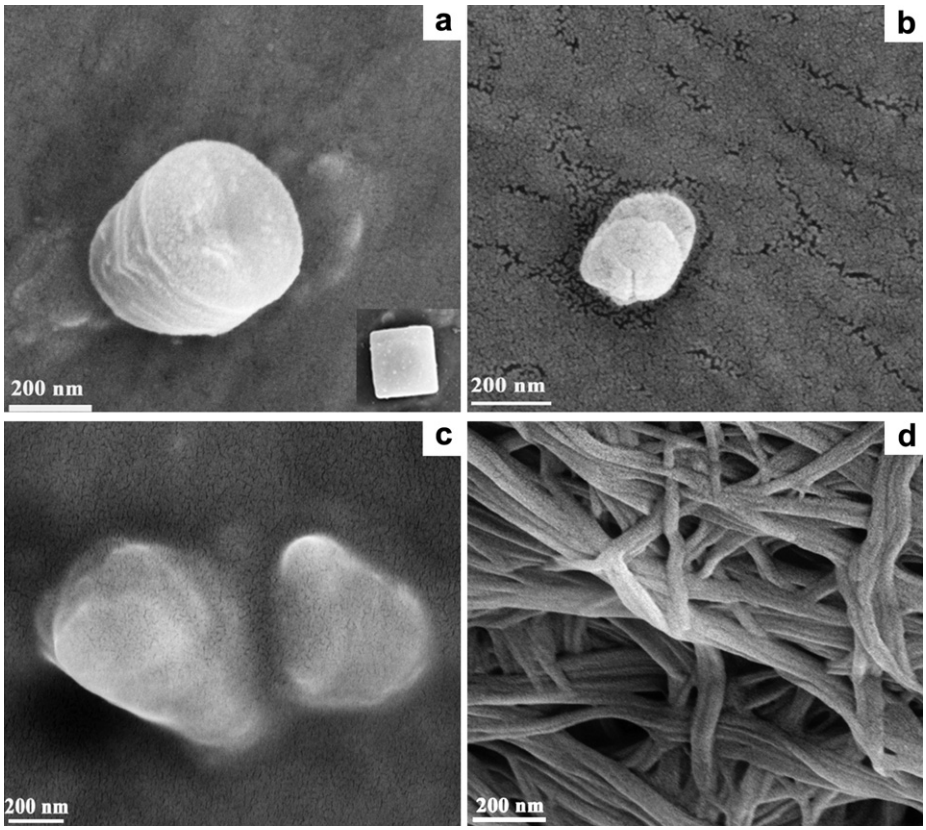

Fig. 9. SEM images of PCTP in $CHCl_3$ (a), PADC in $CHCl_3$ (b) and powder phase of PCTP (c) and PADC (d).

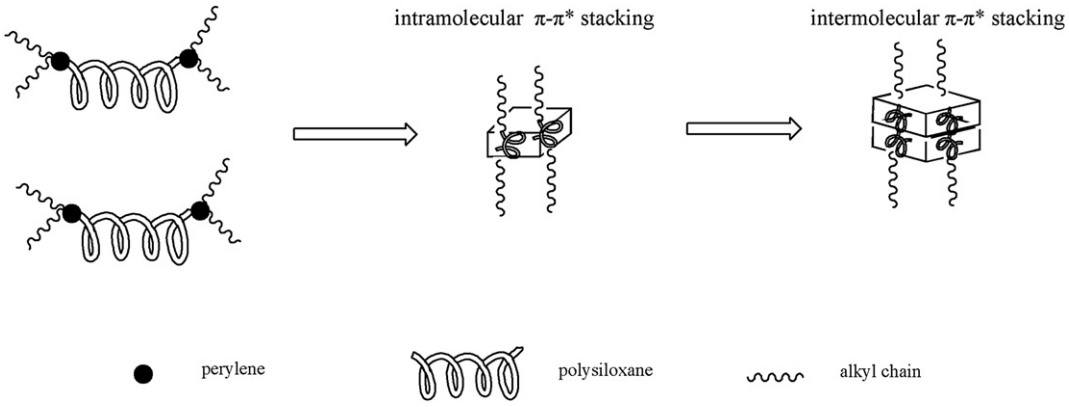

Scheme 2. Schematic diagram of possible mechanism for the different crystal phase formation of PCTP.

Polysiloxane is famous for the chain flexibility, and thus affects PCTP rotated to the favorable direction of $\pi-\pi^*$ stacking. Compared with PADC, PCTP at the same concentration displayed extremely regularly order, and the partial enlarged drawing presented a special crescent-shape [Fig. 8(b) and (c)]. The film thickness of PCTP ranged from 70.47 nm to 112.52 nm, which corresponds to the intramolecular and intermolecular $\pi-\pi^*$ stacking of perylene core.

Furthermore, we studied the morphology of PADC and PCTP films using SEM at room temperature (25 °C). The SEM images in Fig. 9 illustrate some interesting shapes. The images were assigned to PCTP in $CHCl_3$ (a), PADC in $CHCl_3$ (b), and the powder phases of PCTP (c) and PADC (d). The different crystal phases of PCTP were obtained for the intramolecular and intermolecular $\pi-\pi^*$ stacking of the perylene part of PCTP [Fig. 9(a)] [34–37]. On the basis of the AFM images, the possible mechanism for the different crystal phase formation of PCTP was shown in Scheme 2 [38]. The distinct crystal phase was not observed in the powder phase of PCTP [Fig. 9(c)] because the revolution of polysiloxane chain was restricted, and $\pi-\pi^*$ interactions became difficult.

PADC in solution did not exhibit an orderly structure in contrast to PCTP in solution. The results demonstrated that PCTP with flexible polysiloxane chain promoted the appearance of $\pi-\pi^*$ stacking. For powder phase of PADC, $\pi-\pi^*$ favored one-dimensional growth and mainly revealed a belt-like phase [34]. According to the comparison between PADC and PCTP, the presence of Si–O–Si chain provided a force to promote $\pi-\pi^*$ stacking appearance because the chain was flexible, thereby allowing the perylene core to rotate at any angle and form $\pi-\pi^*$ stacking.

4. Conclusion

In summary, we successfully synthesized a novel material with excellent properties. PCTP exhibited an excellent optical property compared with ATP. PCTP exhibited a liquid-crystalline property, which can be attributed to the presence of $\pi-\pi^*$ stacking between adjacent perylene cores. This result was confirmed via DSC, POM, XRD, and SAXS. The crystal phase was observed from the AFM and SEM images, and the possible mechanism for the different phase formation was revealed. PCTP also exhibited great thermal stability and excellent hydrophobic property, which can improve the applications of perylene derivatives. Based on these special properties, PCTP could be used as a hydrophobic liquid-crystalline material at the temperatures ranged from 27.1 °C to 61.3 °C. These properties suggest that the modified perylene derivative can be a promising candidate for organic electronic applications.

Acknowledgments

This work was financially supported by the National Natural Science Foundation of China (No. 20874057) and the Key Natural Science Foundation of Shandong Province of China (No. ZR2011BZ001).

References

[1] Kufazvinei C, Ruether M, Wang J, Blau W. A blue light emitting perylene derivative with improved solubility and aggregation control: synthesis, characterisation and optical limiting properties. Org Electron 2009;10(4):674–80.
[2] Haas U, Thalacker C, Adams J, Fuhrmann J, Riethmuller S, Beginn U, et al. Fabrication and fluorescence properties of perylene bisimide dye aggregates bound to gold surfaces and nanopatterns. J Mater Chem 2003;13(4):767–72.
[3] He X, Liu H, Li Y, Wang S, Wang N, Xiao J, et al. Gold nanoparticle-based fluorometric and colorimetric sensing of copper(II) ions. Adv Mater 2005;17(23):2811–5.
[4] Keuker-Baumann S, Bock H, Sala FD, Benning SA, Haßheider T, Frauenheim T, et al. Absorption and luminescence spectra of electroluminescent liquid crystals with triphenylene, pyrene and perylene units. Liq Cryst 2001;28(7):1105–13.
[5] Shi M-M, Chen H-Z, Sun J-Z, Ye J, Wang M. Fluoroperylene diimide: a soluble and air-stable electron acceptor. Chem Commun 2003;14:1710–1.
[6] Horowitz G, Kouki F, Spearman P, Fichou D, Nogues C, Pan X, et al. Evidence for n-type conduction in a perylene tetracarboxylic diimide derivative. Adv Mater 1996;8(3):242–5.
[7] Law KY. Organic photoconductive materials: recent trends and developments. Chem Rev 1993;93(1):449–86.
[8] Mo X, Chen H-Z, Shi M-M, Wang M. Syntheses and aggregate behaviors of liquid crystalline alkoxycarbonyl substituted perylenes. Chem Phys Lett 2006;417(4–6):457–60.
[9] Wicklein A, Muth M-A, Thelakkat M. Room temperature liquid crystalline perylene diester benzimidazoles with extended absorption. J Mater Chem 2010;20(39):8646–52.
[10] Jancy B, Asha SK. Control of molecular structure in the generation of highly luminescent liquid crystalline perylenebisimide derivatives: synthesis, liquid crystalline and photophysical properties. J Phys Chem B 2006;110(42):20937–47.
[11] Avlasevich Y, Li C, Mullen K. Synthesis and applications of core-enlarged perylene dyes. J Mater Chem 2010;20(19):3814–26.
[12] Muth M-A, Carrasco-Orozco M, Thelakkat M. Liquid-crystalline perylene diester polymers with tunable charge-carrier mobility. Adv Funct Mater 2011;21(23):4510–8.
[13] Hertmanowski R, Biadasz A, Martyński T, Bauman D. Optical spectroscopy study of some 3,4,9,10-tetra-(*n*-alkoxy-carbonyl)-perylenes in Langmuir–-Blodgett films. J Mol Struct 2003;646(1–3):25–33.
[14] Hassheider T, Benning SA, Kitzerow H-S, Achard M-F, Bock H. Color-tuned electroluminescence from columnar liquid crystalline alkyl arenecarboxylates. Angew Chem Int Ed 2001;40(11):2060–3.
[15] Yang L, Shi M, Wang M, Chen H. Synthesis, electrochemical, and spectroscopic properties of soluble perylene monoimide diesters. Tetrahedron 2008;64(22):5404–9.
[16] Zhang X, Wu Y, Li J, Li F, Li M. Synthesis and characterization of perylene tetracarboxylic bisester monoimide derivatives. Dyes Pigm 2008;76(3):810–6.

[17] Xue C, Sun R, Annab R, Abadi D, Jin S. Perylene monoanhydride diester: a versatile intermediate for the synthesis of unsymmetrically substituted perylene tetracarboxylic derivatives. Tetrahedron Lett 2009;50(8):853–6.
[18] Lai Q, Lu H, Wang D, Wang H, Feng S, Zhang J. Color-tunable luminescent materials based on functional polysiloxane and lanthanide ions. Macromol Chem Phys 2011;212(14):1435–42.
[19] Benning S, Kitzerow HS, Bock H, Achard MF. Fluorescent columnar liquid crystalline 3,4,9,10-tetra-(*n*-alkoxycarbonyl)-perylenes. Liq Cryst 2000;27(7):901–6.
[20] Guihua Fu MW, Wang Yongliang, Xia Nan, Wang Wei, Burger Christian. Ionic self-assembled derivatives of perylenetetracarboxylic dianhydride: facile synthesis, morphology and structures. New J Chem 2009;33:784–92.
[21] Liang Y, Wang D, Wu Y, Lai Q, Xue L, Feng S. Perylene-containing polysiloxane: an effective candidate for corrosion protection of iron surface. Appl Surf Sci 2011;257(24):10576–80.
[22] Schouwink P, Schäfer AH, Seidel C, Fuchs H. The influence of molecular aggregation on the device properties of organic light emitting diodes. Thin Solid Films 2000;372(1–2):163–8.
[23] Kohl C, Weil T, Qu J, Müllen K. Towards highly fluorescent and water-soluble perylene dyes. Chem Eur J 2004;10(21):5297–310.
[24] Würthner F, Thalacker C, Diele S, Tschierske C. Fluorescent J-type aggregates and thermotropic columnar mesophases of perylene bisimide dyes. Chem Eur J 2001;7(10):2245–53.
[25] Shin WS, Jeong H-H, Kim M-K, Jin S-H, Kim M-R, Lee J-K, et al. Effects of functional groups at perylene diimide derivatives on organic photovoltaic device application. J Mater Chem 2006;16(4):384–90.
[26] Han JTLD, Ryu CY, Cho K. Fabrication of superhydrophobic surface from a supramolecular organosilane with quadruple hydrogen bonding. J Am Chem Soc 2004;126(15):4796–7.
[27] Laschat S, Baro A, Steinke N, Giesselmann F, Hägele C, Scalia G, et al. Discotic liquid crystals: from tailor-made synthesis to plastic electronics. Angew Chem Int Ed 2007;46(26):4832–87.
[28] Van der Boom T, Hayes RT, Zhao Y, Bushard PJ, Weiss EA, Wasielewski MR. Charge transport in photofunctional nanoparticles self-assembled from zinc 5,10,15,20-tetrakis(perylenediimide)porphyrin building blocks. J Am Chem Soc 2002;124(32):9582–90.
[29] Hae-Ryong Chung EK, Oikawa Hidetoshi, Kasai Hitoshi, Nakanishi Hachiro. Effect of solvent on organicnanocrystal growth using the reprecipitation method. J Cryst Growth 2006;294:459–63.
[30] Wicklein A, Lang A, Muth M, Thelakkat M. Swallow-tail substituted liquid crystalline perylene bisimides: synthesis and thermotropic properties. J Am Chem Soc 2009;131(40):14442–53.
[31] Fairclough JPA, SC, Ryan AJ, Hamley IW, Daniel C, Helsby WI. Correlation of lattice deformation with macroscopic strain for the hexagonal-packed cylinder phase of a triblock copolymer. Polymer 2000;41(7):2577–82.
[32] Rodríguez-Abreu CA-TC, Solans C, López-Quintela A, Tiddy GJT. Characterization of perylene diimide dye self-assemblies and their use as templates for the synthesis of hybrid and supermicroporous nanotubules. ACS Appl Mater Interfaces 2011;3(10):4133–41.
[33] Witte GHK, Söhnchen S, Wöll C. Growth and morphology of thin films of aromatic molecules on metals: the case of perylene. Appl Phys A Mater Sci Process 2006;82(3):447–55.
[34] Balakrishnan K, Datar A, Oitker R, Chen H, Zuo J, Zang L. Nanobelt self-assembly from an organic n-type semiconductor: propoxyethyl-PTCDI. J Am Chem Soc 2005;127(30):10496–7.
[35] Balakrishnan K, Datar A, Naddo T, Huang J, Oitker R, Yen M, et al. Effect of side-chain substituents on self-assembly of perylene diimide molecules: morphology control. J Am Chem Soc 2006;128(22):7390–8.
[36] Datar A, Balakrishnan K, Yang X, Zuo X, Huang J, Oitker R, et al. Linearly polarized emission of an organic semiconductor nanobelt. J Phys Chem B 2006;110(25):12327–32.
[37] Zhang X, Zhang X, Zou K, Lee C-S, Lee S-T. Single-crystal nanoribbons, nanotubes, and nanowires from intramolecular charge-transfer organic molecules. J Am Chem Soc 2007;129(12):3527–32.
[38] Lei Y, Liao Q, Fu H, Yao J. Phase- and shape-controlled synthesis of single crystalline perylene nanosheets and its optical properties. J Phys Chem C 2009;113(23):10038–43.